The 2009 IEEE/RSJ International Conference on
Intelligent Robots and Systems
October 11-15, 2009 St. Louis, USA

Microassembly of Complex and Solid 3D MEMS by 3D Vision-based Control

Brahim Tamadazte, Nadine Le Fort-Piat
Sounkalo Dembélé,
FEMTO-ST Institute, -AS2M-, UMR CNRS
6174 - UFC / ENSMM / UTBM
24 rue Alain Savary, 25000 Besançon, France
Emails : {btamadaz, npiat, sdembele}@ens2m.fr

Eric Marchand
INRIA Rennes-Bretagne Atlantique
IRISA, Lagadic
Email : eric.marchand@irisa.fr

Abstract— **This paper describes the vision-based methods developed for assembly of complex and solid 3D MEMS (micro electromechanical systems) structures. The microassembly process is based on sequential robotic operations such as planar positioning, gripping, orientation in space and insertion tasks. Each of these microassembly tasks is performed using a pose-based visual control. To be able to control the microassembly process, a 3D model-based tracker is used. This tracker is able to directly provide the 3D micro-object pose at real-time and from only a single view of the scene. The methods proposed in this paper are validated on an automatic assembly of fives silicon microparts of 400 μm $\times$ 400 μm $\times$ 100 μm on 3-levels. The insertion tolerance (mechanical play) is estimated to 3 μm. The precision of this insertion tolerance allows us to obtain solid and complex micro electromechanical structures without any external joining (glue, wending. Promising positioning and orientation accuracies are obtained who can reach 0.3 μm in position and 0.2° in orientation.**

I. Introduction

Fabrication of complex miniature sensor and actuator systems, hybrid Micro Electro Mechanical Systems (MEMS) or Micro Opto Electro Mechanical Systems (MOEMS) devices are gaining popularity. In the last decade, researches have been deliberately oriented towards the development of microrobotic cells to assist the human operator to handle or assemble such microparts, [3], [2], [17], [5]. In contrast to self-assembly [19], robotic microassembly is directed and deterministic and based on serial [22] or parallel [7] approaches. Recently, automation of microassembly tasks are one of ultimate goals. Meanwhile, the availability of high resolution cameras and powerful microprocessors have made possible for the vision systems to play a key role in the automatic microsystems assembly field. Therefore, vision sensor is essential to perform microhandling tasks, even in tele-operated mode and indispensable for automatic mode. Several vision techniques have been successfully implemented in the microdomain. It was shown that vision feedback control is an appropriate solution in automation of microhandling and microassembly tasks [18], [6], [11], [12]. Among tasks studied and described in the literature concerning automated assembly, we can cite the microassembly of type of peg-into-hole or 2D1/2 realization by stacking planar thin layers. In this paper, we focus on 3D complex robotic (serial) microassembly of silicon microcomponents. The microparts size is 400 $\times$ 400 $\times$ 100 μm^3. These silicon microcomponents are assembled in aim to built a complex and solid 3-levels microstructure using pose-based visual servoing (PBVS). The choice of using 3D vision feedback control leads to use a 3D model-based tracker that is able to directly provide the 3D object pose. These 3D poses are computed using just a single view of the scene. It is in this context that the algorithm *VIsual Servoing Platform* (VISP) developed by Marchand and his coworkers [1], [16] is used to perform the complex assembly presented in this paper.

This paper is structured as followed: section II describes the robotic cell used to validate the techniques developed. Section III presents the assembly process to perform. Section IV, illustrates the control law implemented to achieve the assembly of five microparts using a 3D model-based tracking. Section V presents some experimental results obtained and discussions about these results.

II. Experimental setup

A. Microrobotic cell

The robotic cell which is developed to validate the concepts proposed in this paper, includes a mechanical system of five degree of freedom (dof), a gripping system of four dof and an imaging system. The microassembly station is located inside a controlled environment (laminar flow hood) and posed on a vibration-free table. Two PCs connected by an Ethernet link process the informations, the first (Pentium (R) D, CPU 2.80 G Hz, 2 Go of RAM) is dedicated for vision algorithms while the second (Pentium(R) 4, CPU 3.00 G Hz, and 1 Go of RAM) is used for control algorithms. The five dof of the workcell are decomposed on three dof xyθ (two high accuracy linear stages *xy* and one high rotation stage θ) for the positioning platform and two dof zϕ (one vertical linear stage z and one rotation stage ϕ tilted at 45 $^\circ$ from the vertical axis) for the micromanipulator. The resolution of the translations stages is 0.007 μm and 26 μrad for the rotation stages (all from Polytec PI). The positioning platform is equipped with a compliant table (the table is supported by three springs) and enables the positioning in the horizontal plane. The manipulator supports the gripping system and

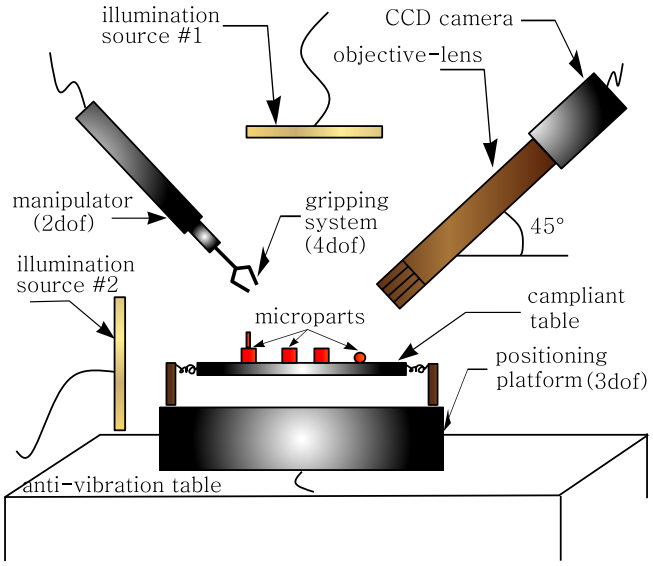

Fig. 1. The configuration of the microrobotic cell

enables the vertical positioning and spatial orientation of microparts. CCD camera is used for imaging and it associate 11.452 mm focal-length lens and a 140 mm tube. It is tilted at 45 ° from the horizontal plane in order to ensure a better view (perspective view during the assembly tasks) of the scene (Fig. 1). The image format is 1280 × 960 pixels enabling an acquisition frequency of 7.5 images per second. The other specifications are: resolution of 0.95 μm, working distance of 80 mm, field-of-view of 1.216 mm × 0.912 mm. The camera is mounted on *xyz* manual translation stages.

B. Manipulated micro-object

The availability of micro fabrication technologies enables machining microparts which can be used as building blocks for microsystems. Released structures etched on silicon wafer are mounted on mechanical play using engraved notches. These microparts can be inserted each other to achieve stable 3D structures without using any fixing process. Figure 2 shows the CAD (computer aided design) model with the corresponding dimensions of some samples. During the microassembly process, the microparts are placed on sticky surface.

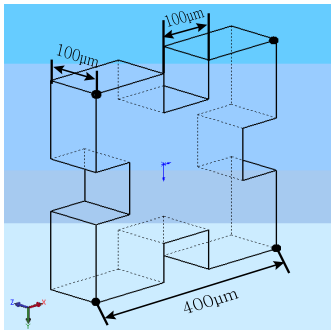

Fig. 2. The CAD (computer aided design) model of the MEMS microstructure

III. Microassembly processes

Microassembly i.e. assembly of MEMS is a delicate operation because in addition to the planar positioning and orientations tasks required for the MEMS handling, it requires more complicated operations like space orientation of the microparts and insertion tasks. The latter represents the fitting together of two or more single MEMS in order to build a 3D solid microstructure. So, it is more natural to use a pose-based visual servoing approach (also known as 3D visual control) when the 3D pose of the object tracked is known. The main advantage is that task is described as a regulation to zero of 3D error (between the position of two microparts to assemble). Until now, few publications [8], [23] had investigated the microassembly by implementation of 3D visual control.

Let us consider the objective to assemble five simple MEMS [**A**, **B**, **C**, **D** and **E**] to build a complex and solid 3D MEMS as illustrated by Fig. 6.h. The insertion tolerance of two parts is less than 3 μm. The assembly problem of these microparts is structured as followed:

IV. Modelling process

A. CAD model tracking

To track the microscale object, it is considered a 3D model-based tracker that allows the computation of the object pose. It relies full-scale non-linear optimization techniques [9], [13], [4], [1] which consists of minimizing the error between the observation and the forward-projection of the model. In this case, minimization is handled using numerical iterative algorithms such as Newton-Raphson or Levenberg-Marquardt. Let us note that such tracker have also been consider in the case of microsystems in [23].

The goal of tracker is to compute the position ${}^{c}\mathbf{M}_{o}$ of the object in the camera frame[1]. In this paper, the pose computation is formulated in terms of a full-scale non-linear optimization: *Virtual Visual Servoing* (VVS). In this way the pose computation problem is considered as similar to 2D visual servoing as proposed in [1]. Assuming that the low level data extracted from the images are likely to be corrupted, a statistically robust camera pose estimation process based on the widely accepted statistical techniques of robust M-estimation [10] is used. This M-estimation is directly introduced in the control law to address [1]. This framework is used to create an image feature based system which is capable of treating complex scenes in real-time.

More precisely, we minimize the distances between contour points extracted from the image and the projection of the 3D lines of the CAD model of the object (see Fig. 3).

[1]Let us define the rigid transformation between a frame $\mathscr{R}_a$ and a frame $\mathscr{R}_b$ by an homogeneous matrix ${}^{a}\mathbf{M}_{b}$ defined by:

$$ {}^{a}\mathbf{M}_{b} = \begin{bmatrix} {}^{a}\mathbf{R}_{b} & {}^{a}\mathbf{t}_{b} \\ 0 & 1 \end{bmatrix}, \tag{1} $$

where ${}^{a}\mathbf{R}_{b}$ is the rotation matrix and ${}^{a}\mathbf{t}_{b}$ the translation vector. It is also possible to note the pose by the vector ${}^{a}\mathbf{r}_{b} = ({}^{a}\mathbf{t}_{b}, \theta\mathbf{u})$ where $\theta\mathbf{u}$ is the axes and the angle of the rotation.

Algorithm 1: The algorithm structure used to assemble 3D-solid MEMS

begin
  Initialization of the tracker
  for i = *1:5* **do**
1 **if** i = *1* **then**
    - tracking and planar positioning of **A**
    - gripping and placing **A**
    - tracking and planar positioning of **B**
    - gripping **B**
  compute automatically the desired position of **B**
2 **if** i = *2* **then**
    - tracking, spatial positioning and placing **B**
    - tracking and planar positioning of **C**
    - gripping **C**
  compute automatically the desired position of **C**
3 **if** i = *3* **then**
    - tracking **A** and planar positioning of **[A+B]**
    - tracking, spatial positioning and insertion of **C** into **[A+B]**
  compute automatically the desired position of **D**
4 **if** i = *4* **then**
    - tracking and positioning of **D**
    - gripping **D**
    - tracking **A**, spatial positioning and insertion of **D** into **[A+B+C]**
  compute automatically the desired position of **E**
5 **if** i = *5* **then**
    - tracking and planar positioning of **E**
    - gripping **E**
    - tracking **A**, planar positioning **[A+B+C+D]**
    - tracking **E**, spatial positioning and insertion of **E** into **[A+B+C+D]**
end

Let us denote $\mathbf{p}_i, i = 1..k$ these points and $\mathbf{l}_i(\mathbf{r})$ the projection of the corresponding line for the pose $\mathbf{r}$.

$$\widehat{{}^{c}\mathbf{M}_o} = \arg\min_{{}^{c}\mathbf{R}_o, {}^{c}\mathbf{t}_o} \sum_{i=1}^{k} \rho\left(d_{\perp}(\mathbf{p}_i, \mathbf{l}_i({}^{c}\mathbf{r}_o))\right) \tag{2}$$

where $\rho(.)$ is the robust function that allows to handle corrupted data. The distance $d_{\perp}(.)$ is represented on Fig. 4

Since a Gauss-Newton approach is considered to minimize equation (2) a Jacobian has to be defined and is given in [1].

B. Position-based visual servo for microassembly

Position-based control schemes (PBVS) [21], [20] use the pose of the camera with respect to some reference coordinate frame to define $\mathbf{s}$. This 3D pose is computed using the 3D model-based tracking presented in the previous section. It is convenient to consider three coordinate frames: the current camera (optical microscope) frame ($\mathscr{R}_c$), the desired camera frame ($\mathscr{R}_{c*}$) and the reference frame ($\mathscr{R}_{oi}$) attached to each microparts (i = *1 to 5*) to assemble. Let ${}^{c}\mathbf{t}_o$ and ${}^{c*}\mathbf{t}_o$ be

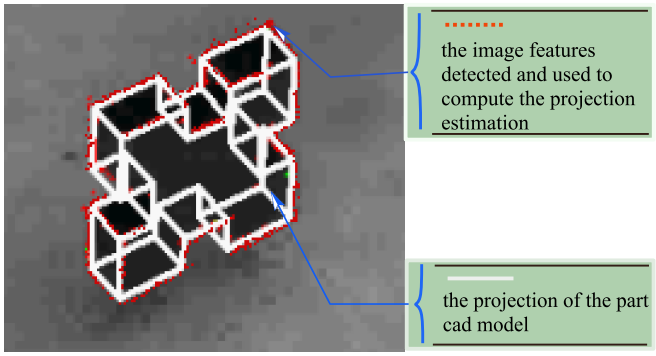

Fig. 3. The points drawn in red are used for determining the image features which are used in the calculation of the projection estimation of the CAD model. The straights lines of the CAD model are drawn in white color.

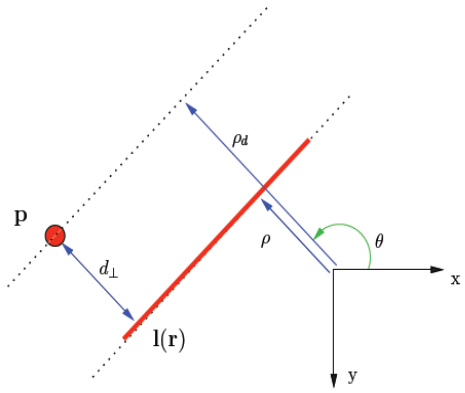

Fig. 4. Distance of a point to a line

the coordinates of the origin of each micro-object frame relative to the current camera frame and the origin of each micro-object frame relative to the desired camera frame. Furthermore, Let ${}^{c*}\mathbf{R}_c$ be the rotation matrix that defines the orientation between the current camera frame and the desired camera frame.

It can define $\mathbf{s}$ to be ($\mathbf{t}$, $\theta\mathbf{u}$), in which $\mathbf{t}$ is a translation vector, and $\theta\mathbf{u}$ gives the angle/axis parameterization for the rotation.

To express the control law in the fixed frame linked to the robotic cell, it is necessary to find the homogeneous transformation ${}^{\mathscr{F}}\mathbf{M}_c$ between the camera frame ($\mathscr{R}_c$) and the workcell frame ($\mathscr{R}_{\mathscr{F}}$). Therefore, for each micropart (i), the homogeneous transformation ${}^{\mathscr{F}}\mathbf{M}_i$ can be computed as:

$${}^{\mathscr{F}}\mathbf{M}_i = {}^{\mathscr{F}}\mathbf{M}_c \, {}^{c}\mathbf{M}_i \tag{3}$$

where ${}^{\mathscr{F}}\mathbf{M}_c$ is the position of the camera in the reference frame of the workcell (which is a known constant) and ${}^{c}\mathbf{M}_i$ is given by the CAD model-based tracking algorithm.

So, it can define the 3D pose (current pose and desired pose) of a micro-object (i) in the workcell frame $\mathscr{R}_{\mathscr{F}}$, respectively, by

$$\mathbf{s}_i = ({}^{\mathcal{F}}\mathbf{t}_i,\ \theta\mathbf{u}), \tag{4}$$

$$\mathbf{s}_i^* = ({}^{\mathcal{F}}\mathbf{t}_{i^*},\ 0), \tag{5}$$

The aim of all vision-based control schemes is to minimize the error $\mathbf{e}$ defined by

$$\mathbf{e}_i = ({}^{\mathcal{F}}\mathbf{t}_{i^*} - {}^{\mathcal{F}}\mathbf{t}_i,\ \theta\mathbf{u}), \tag{6}$$

And if we would like for instance to try to ensure an exponential decrease of the error $\mathbf{e}$, we write

$$\dot{\mathbf{e}}_i = -\lambda\mathbf{e} \tag{7}$$

To improve the convergence rate, it have implemented an adaptive gain (the gain increases when the error decreases):

$$\lambda = (\lambda_{max} - \lambda_{min})exp^{-\kappa\|\mathbf{e}\|} + \lambda_{min} \tag{8}$$

where $\lambda_{\max}$ and $\lambda_{\min}$ are the maximum and minimum values of λ, respectively. The parameter κ allows the tuning of the decreasing rate of the error exponential decrease.

The equation that links the variation $\dot{\mathbf{s}}_i$ of the visual feature $\mathbf{s}_i$ to the robot velocity in the robot reference frame $(v,\omega)^\top_{\mathcal{F}}$ is given by [15]

$$\begin{pmatrix} {}^{\mathcal{F}}\dot{\mathbf{t}}_i \\ \dot{\theta\mathbf{u}} \end{pmatrix} = \begin{pmatrix} \mathbf{I}_{3\times3} & \mathbf{0}_{3\times3} \\ \mathbf{0}_{3\times3} & \mathbf{J}_\omega \end{pmatrix} \begin{pmatrix} v \\ \omega \end{pmatrix}_{\mathcal{F}} \tag{9}$$

where

$$\mathbf{J}_\omega = \mathbf{L}_\omega {}^c\mathbf{R}_{\mathcal{F}} \tag{10}$$

where $\mathbf{L}_\omega$ is such that $\mathbf{L}_\omega^{-1}\theta\mathbf{u} = \theta\mathbf{u}$ [14].

The control scheme is obtained with following relationship:

$$\mathbf{v} = \lambda\mathbf{J}_\omega^{-1}\mathbf{e} \tag{11}$$

The switch between the different tasks of positioning (control of the positioning platform) and insertion (control of the micromanipulator) for successive microparts is done when the threshold of translation and rotation error is reached ($\|\mathbf{e}_t\| < \delta_1$ (μm) and $\|\mathbf{e}_r\| < \delta_2$ (°)). The same threshold is applied for all the microassembly process tasks.

The desired position of the first micropart **A** is defined manually (${}^{\mathcal{F}}\mathbf{M}_A$) (initialization step). When **A** is perfectly positioned ($\|\mathbf{e}_t\| < \delta_1$ and $\|\mathbf{e}_r\| < \delta_2$), the final position of the second micropart is computed automatically by

$${}^{\mathcal{F}}\mathbf{M}_i = {}^{\mathcal{F}}\mathbf{M}_A\ {}^A\mathbf{M}_i \tag{12}$$

with i the micropart label (**A**, **B**, **C**, **D** or **E**) and ${}^A\mathbf{M}_i$ represents the transformation matrix between the frame linked to the micropart **A** to the frame linked to the micropart i. For example, the passage matrix between the desired pose of the micropart **A** and the desired pose of the micropart (see Fig. 5) **B** is given by

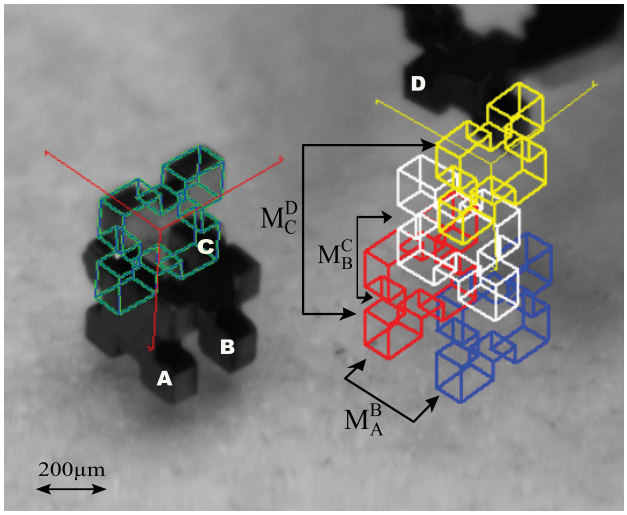

Fig. 5. The image illustrates an intermediate step of the microassembly process. This step represents the positioning task of the micropart **C** under the gripper system followed by the insertion task of the micropart **D** into **[A+B+C]**.

$${}^A\mathbf{M}_B = \begin{pmatrix} 1 & 0 & 0 & 0 \\ 0 & 1 & 0 & 0 \\ 0 & 0 & 1 & 300 \\ 0 & 0 & 0 & 1 \end{pmatrix} (\mu m) \tag{13}$$

V. Results and Discussions

A. Assembly without external joining

Figure 6 illustrates a sequence of images from the optical videomicroscope system showing the process of the automatic microassembly of five silicon microparts of size of 400 × 400 × 100 μm^3. Figure 6.a illustrates the first step which concerns the tracking and the positioning of micropart **A**. Figure. 6.b represents the tracking and placing of micropart **B**. Figure 6.c shows the tracking of the micropart **A** and the positioning of the both microparts **[A+B]**. Figure 6.d shows the tracking and insertion of the micropart **C** into the microparts **[A+B]**. Figure 6.e represents the tracking of the micropart **A** and the positioning of the microparts **[A+B+C]**. Figure 6.f illustrates the tracking and the insertion of the micropart **D** into the microparts **[A+B+C]**. Figure 6.g shows the end of the assembly process which concerns the insertion of the fifth micropart into **[A+B+C+D]**. Figure 6.h represents the zooming into the final solid 3D microassembly performed.

B. Assembly precision and cycle time

A set of experiments was performed to determine the precision of the visual tracking system as well as of the pose-based visual control implemented. Although the precision of measurements is dependent on various factors as for example the degree of the image sharpness. Despite the visualization partially blur of the microparts during the assembly process,

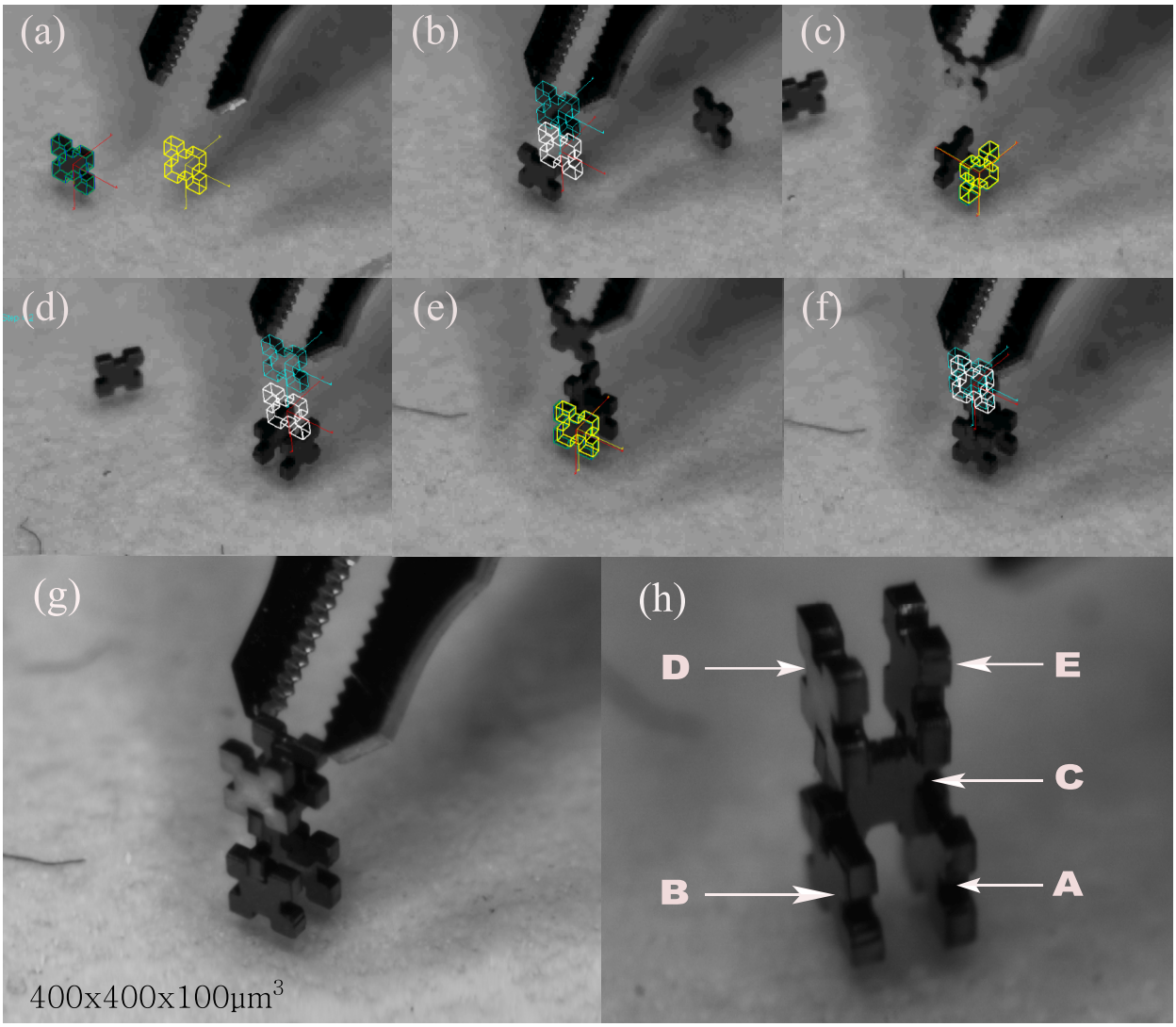

Fig. 6. Sequence of images captured during the microassembly process

the tracker remains efficient. Therefore, combined with the pose-based visual servo, we get a high-precision during the positioning and orientation tasks (translation error reaches 0.3 μm and orientation error reaches 0.2°) which are obtained by the encoders of the different angular and linear motions. These results have led to obtain a solid assembly as shown in Fig. 7.

The time spent to achieve a single MEMS assembly (assembly of two silicon microparts) is computed. The average time required is about 41 seconds which is an exceptional value for this kind of task. It is important to emphasize that the mean cycle time for the same assembly performed by a human operator is about 10 minutes if this person has approximately one month of training using a teleoperation system (joystick). With such a time, it is almost impossible to make the product beneficial contrary to the automatic mode.

VI. Conclusion

Hybrid microsystems and microassembly technologies are under rapid development as well as the industrial and market potential are growing. The main bolt which suffers the microsystem field is the microassembly. Therefore, advances in the microassembly field can be expected to have an important impact on the MEMS production volume, their complexity (number of microcomponents composing the MEMS), the continuity on their miniaturization. Automation of the current manual microassembly processes is a way to more precise assembly, higher productivity and more fast. It is in this context that the works presented in this paper investigate a new microassembly approach. In aim to validate the concepts defined, a microrobotic cell has been developed. It consists of a high resolution five degree of freedom: three dof for the positioning platform and two dof the micromanipulator. Through the approaches presented in this paper, it is demonstrated the possibility to achieve automatic microassembly of solid and complex 3D MEMS on 3-levels using pose-based visual controls. The most advantages of these approaches are that assembly task of two microparts is described as a 3D error (between the current 3D pose and the desired

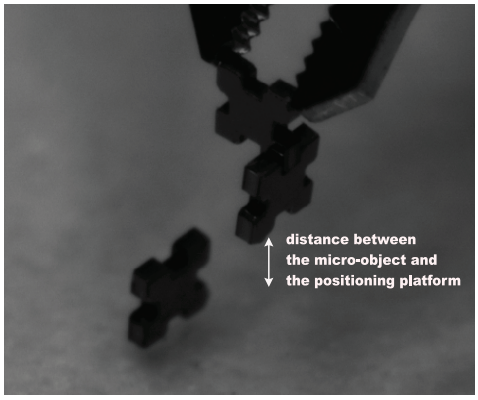

Fig. 7. The image shows the strength of an assembly of two microparts without external joining, it is due to the low microparts insertion tolerance (about 3 μm).

3D pose of two microparts to assemble) to be regulated to zero. The complete assembly MEMS tasks is decomposed on multiple subtasks performed sequentially: positioning, gripping, orientation, placing and insertion. Each of these subtasks is performed automatically. A high precision is obtained during the assembly process, and reached 0.3 μm in position and 0.2 $^\circ$ in orientation.

To be able to control the microassembly process, it is necessary to track the microscale object to be assembled over frames during the experiment. Therefore, we decided to use a 3D model-based tracker that is able to directly provide the 3D micro-object pose in real-time using only a single view of the scene. There are several advantages to use CAD models as a standard form of inputs for a flexible automation system. It has been proved that the CAD model-based tracking is essential for robust and accuracy microscale visual servoing system. For example, it is more efficient during partial occlusions of tracked micro-objects by the gripper or other micro-objects.

We had validated the approaches proposed in this paper by an assembly of five of 400 μm $\times$ 400 μm $\times$ 100 μm silicon microparts. These microcomponents are assembled by their 100 μm $\times$ 100 μm $\times$ 100 μm notches with a mechanical play (insertion tolerance) of 3 μm. This low tolerance allows to assemble securely these microparts without external joining.

AKNOWLEDGEMENTS

This work is partially conducted with financial support from the project Hybrid Ultra Precision Manufacturing Process Based on Positional and Self assembly for Complex Micro-Products (HYDROMEL NMP2-CT-2006-026622) funded by the European Commission.

REFERENCES

[1] A.I. Comport, E. Marchand, M. Pressigout, and F. Chaumette, *Real-time markerless tracking for augmented reality: the virtual visual servoing framework*, IEEE Transactions on Visualization and Computer Graphics, vol.**12**, (2006), no. 4, pp. 615–628.

[2] A.N. Das, Ping Zhang, W.H. Lee, D. Popa, and H. Stephanou, *μ3: Multiscale, deterministic micro-nano assembly system for construction of on-wafer microrobots*, IEEE International Conference on Robotics and Automation, (Rome, Italy), (april, 2007), pp. 461–466.

[3] N. Dechev, L. Ren, W. Liu, W.L. Cleghorn, and J.K. Mills, *Development of a 6 degree of freedom robotic micromanipulation for use in 3d mems microassembly*, IEEE International Conference on Robotics and Automation, (Orlando, Fl., USA), (may, 2006), pp. 281–288.

[4] T. Drummond and R. Cipolla, *Real-time visual tracking of complex structures*, IEEE Transactions on Pattern Analysis and Machine Intelligence, vol. **24**, (2002), no. 7, pp. 932–946.

[5] S. Fatikow, J. Seyfried, ST. Fahlbuschand A. Buerkle, and F. Schmoeckel, *A flexible microrobot-based microassembly station*, Journal of Intelligent and Robotic Systems, vol. **27**, (2000), pp. 135–169.

[6] Sergej Fatikow, Axel Buerkle, and Joerg Seyfried, *Automatic control system of a microrobot-based microassembly station using computer vision*, SPIE conference on Microrobotics and Microassembly (Boston, Massachusetts, USA), vol. **3834**, (1999), pp. 11–22.

[7] John T. Feddema and Todd R. Christenson, *Parallel assembly of high aspect ration microstructures*, SPIE, Conference on Microrobotics and Microassembly, (Boston, Massachusetts, USA), (september, 1999), pp. 153–164.

[8] John T. Feddema and Ronald W. Simon, *Visual servoing and cad-driven microassembly*, IEEE Robotics and Automation Magazine, vol. **5 (4)**, (1998), pp. 18–24.

[9] R. Haralick, H. Joo, C. Lee, X. Zhuang, V Vaidya, and M. Kim, *Pose estimation from corresponding point data*, IEEE Transactions on Systems, Man and Cybernetics, vol. **19**, (1989), no. 6, pp. 1426–1445.

[10] P.-J. Huber, *Robust statistics*, Wiler, New York, (1981).

[11] Pasi Kallio, Quan Zhou, Juha Korpinen, and Heikki Koivo, *Three dimensional position control of a parallel micromanipulator using visual servoing*, Proceedings of SPIE, vol. **4194**, (Microrobotics and Microassembly II), (Boston, USA), (november, 2000), pp. 103-111

[12] Jung H. Kim, Shih-Kang Kuo, and Chia-Hsiang Menq, *An ultra-precision six-axis visual servo-control system*, IEEE Transactions on Robotics, vol. **21 (5)**, (2005), pp. 985–993.

[13] D.G. Lowe, *Fitting parameterized three-dimensional models to images*, IEEE Transactions on Pattern Analysis and Machine Intelligence, vol. **13**, (1991), no. 5, pp. 441–450.

[14] E. Malis, F. Chaumette, and S. Boudet, *2 1/2 D visual servoing*, IEEE Transactions on Robotics and Automation, vol. **15**, (1999), no. 2, pp. 238–250.

[15] E. Marchand, F. Chaumette, F. Spindler, and M. Perrier, *Controlling an uninstrumented manipulator by visual servoing*, The International Journal of Robotics Research (IJRR), vol. **21**, (2002), no. 7, pp. 635–648.

[16] E. Marchand, F. Spindler, and F. Chaumette, *Visp for visual servoing: A generic software platform with a wide class of robot control skills*, IEEE Robotics and Automation Magazine, vol. **12**, (december, 2005), no. 4, pp. 40–52.

[17] M. Probst, R. Borer, and B. J. Nelson, *A microassembly system for manufacturing hybrid mems*, IFTOMM World Congress (Besançon, France), (june 2007).

[18] Stephen Ralis, Barmeshwar Vikramaditya, and Bradley J. Nelson, *Micropositioning of a weakly calibrated microassembly system using coarse-to-fine visual servoing strategies*, IEEE Transactions on Electronics Packaging Manufacturing, vol. **23 (2)**, (2000), pp. 123–131.

[19] Uthara Srinivasan, Dorian Liepmann, and Fellow Roger T. Howe, *Microstructure to substrate self-assembly using capillary forces*, Journal of Microelectromechanical Systems, vol. **10 (1)**, (march, 2001), pp. 17–24.

[20] B. Thuilot, P. Martinet, L. Cordesses, and J. Gallice, *Position based visual servoing : keeping the object in the field of vision*, IEEE International Conference on Robotics and Automation, (Washington, USA), (may, 2002), pp. 1624–1629.

[21] W. Wilson, C. Hulls, and G. Bell, *Relative end-effector control using cartesian position based visual servoing*, vol. **12**, (october, 1996), pp. 684–696.

[22] G. Yang, J. Gaines, and B. Nelson, *A surpervisory wafer-level 3d microassembly system for hybrid mems fabrication*, Journal of Intelligent and Robotic Systems, vol. **37**, (2003), pp. 43–68.

[23] K. Yesin and B. Nelson, *A cad-model based tracking system for visually guided microassembly*, Robotica, vol. **23**, (2005), pp. 409–418.